Desalination and Water Treatment
www.deswater.com

doi: 10.5004/dwt.2019.23344

138 (2019) 248–256
January

New methodology to develop high-resolution rainfall data using weather radar for watershed-scale water quality model

Dong Jin Jeon[a], Yakov A. Pachepsky[a], Bumjo Kim[b], Joon Ha Kim[b,*]

[a]*USDA-ARS, Environmental Microbial and Food Safety Laboratory, 10300 Baltimore Avenue, Building 173, BARC-East, Beltsville, MD, 20705, USA*
[b]*School of Environmental Science and Engineering, Gwangju Institute of Science and Technology (GIST), 261 Cheomdan-gwagiro, Buk-gu, Gwangju 500-712, Republic of Korea, Tel. +82 62 715 3277; Fax: +82 62 715 2434; email: joonkim@gist.ac.kr (J.H. Kim)*

Received 27 August 2018; Accepted 21 October 2018

ABSTRACT

Watershed-scale water quality models are often used for interpreting changes in complex environmental systems. Precipitation is a primary control affecting the output of watershed-scale water quality model, and higher resolution of precipitation data is highly desirable. The objective of this study was to investigate whether the radar rainfall estimates can improve the accuracy of stream flow, TSS load, and TP load simulations with the soil and water assessment tool for high- and low-flow conditions. Yeongsan River watershed (YRW) was selected for this study. This watershed, located south-west of Korean Peninsula, has an area of about 2,938 km^2, and is divided into 25 sub-watersheds. The simulations were conducted under different rainfall datasets: (1) rainfall observations from nine ground rain gauges (GR), (2) 25 corrected radar rainfall estimates (RR), and (3) a combination of nine ground rain gauges and 16 corrected radar rainfall estimates that represent the 16 ungauged sub-watersheds in YRW (GARR). Simulation results under different the rainfall datasets were compared using the Nash–Sutcliffe efficiency coefficient and percentage bias. The prediction of both high and low stream flows using GARR was better than using GR and RR data. The model performance for predicting TSS load was significantly better under GARR data than under GR and RR data. In case of TP, the model performances using RR and GARR data were significantly better than that using GR data. Overall, combining gauge rainfall and corrected radar rainfall led to an improvement in the prediction accuracy for the watershed-scale water quality model.

Keywords: Radar rainfall image; Soil and water assessment tool; Watershed-scale water quality model; Bias correction; Stream flow; TSS load; TP load

1. Introduction

Watershed-scale water quality models are effective science-based tools for interpreting change in complex environmental systems that affect hydrology cycle, soil erosion, and nutrient fate and transport in watersheds [1,2]. These models have been widely used to address societally important problems of environmental management [3–5]. Accurate model-based simulation of hydrology and water quality is beneficial for planning and management of water resources. Currently, many scientists prefer a distributed model because it can represent the watershed systems more accurately by considering the spatial variability of model parameters and input datasets [6].

Distributed models are developed to improve the simulations of hydrological processes. Owing to the increased availability of spatially distributed parameters and input datasets for distributed models, some authors studied the influence of input data characteristics, such as resolution and time step, on the ability of models to reproduce observed output. Geza and McCray [7] compared model performance for stream flow with two different soil data resolutions in a distributed

* Corresponding author.

model; Chaubey et al. [8] examined the effect of a digital elevation model data resolution on the output uncertainty of the distributed model. Apart from the geological input data, precipitation is one of the primary input data for rainfall-runoff simulation and its detailed spatial distribution is required, because the density of rain gauge networks dominantly affects the variability of hydrographs as well as the surface water quality [9,10]. Thus, input datasets from more dense rainfall can improve the model results. To create the spatially dense coverage of precipitation, several studies have explored using weather radar data as an alternative source of ground rainfall observations. Neary et al. [11], and Kalin and Hantush [12] compared rain gauge data and weather radar data and concluded that the use of weather radar rainfall over gauge rainfall did not offer any improvement. In contrast, some studies proved that corrected radar based rainfall datasets in distributed model simulations were useful for estimating stream flows [4,10,13,14]. The contrasting results in application of weather radar data on distributed model represented that the effectiveness of weather radar data varies with the watershed area, precipitation rate, and density of rain gauge networks. Nevertheless, weather radar data are known to be an alternative way to estimate precipitation rate and are used as input data of distributed hydrologic modeling for stream flow prediction at ungauged basins [15,16].

Furthermore, using weather radar data has been particularly successful for predicting high-intensity rainstorm events [17–19]. Watershed-scale water quality models, however, generate data that can be used to estimate other aspects of the watershed functioning, such as biomass of crop and other plants, loss of nutrients to groundwater, availability of nutrients to plants, partitioning of nutrients between surface runoff and infiltration. These aspects of watershed functioning are affected by intermediate and low-intensity precipitation. Evaluating the performance of the watershed-scale water quality model separately for high- and low-intensity rainstorm events may be beneficial to understand the efficiency of the model as a prediction and management tool.

The objective of this work is to: (1) develop a new rainfall input dataset to improve the prediction accuracy of water quality and quantity in a distributed model using weather radar and (2) evaluate the suitability of weather radar data as the source of input data separately for high and low rainstorm events.

2. Methods

2.1. Model description

The soil and water assessment tool (SWAT), developed by the United States Department of Agriculture, has been widely used to evaluate the impact of management and climate on water resources and agricultural chemical yields [20]. The SWAT model is physically based continuous-time model and appropriate for simulating over long time periods of stream flow and nutrient load at the watershed scale. A watershed in a SWAT model is divided into a number of sub-basins, which in turn are subdivided into hydrologic response units (HRUs); each HRU is assumed to have homogeneous land use, slope, and soil type [21]. Physical characteristics such as slopes, reach dimensions, and climate condition were considered for each sub-basin [22]. We used the ArcSWAT2.3.4 of the SWAT2005 version for ArcGIS 9.3 in this study.

2.2. Site description

Yeongsan River watershed (YRW), located south-west of Korean Peninsula, was selected for this study (Fig. 1).

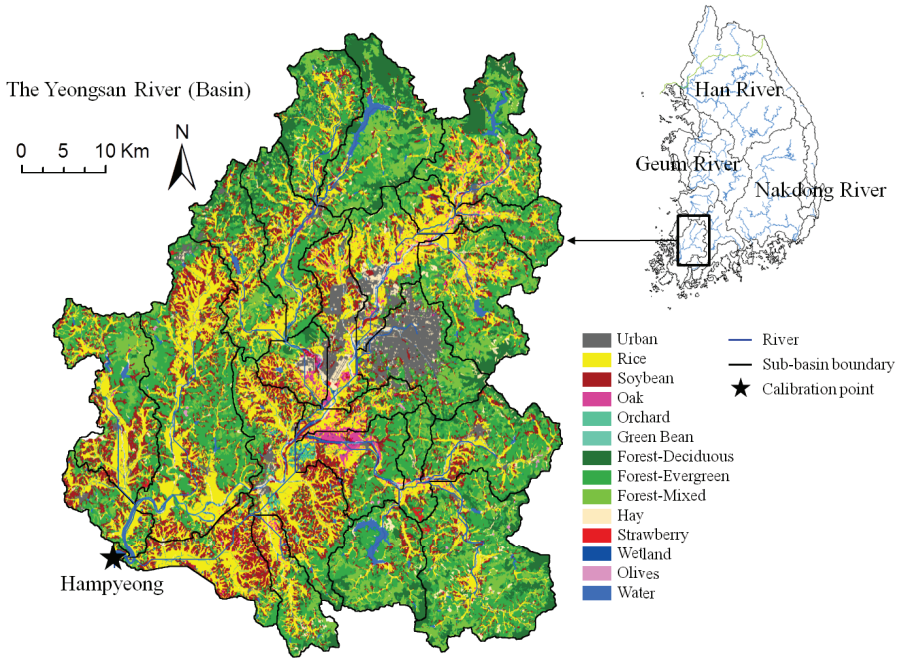

Fig. 1. Land use characteristics of the Yeongsan River watershed in Korea. The final outlet Hampyeong is used as a calibration point.

Yeongsan River (YR) is one of the four major rivers in South Korea. It flows toward the Yellow Sea by passing through Gwangju (GJ), which is the sixth largest metropolitan city. The length of the main stream is 130 km. The delineated watershed has an area of about 2,938 km^2 and is divided into 25 sub-watersheds according to the geophysical conditions and the differentiation laws of the landscapes. The land use within this watershed primarily includes forestry (54%) and agriculture (40%), and the rest is urban. The dominant agricultural crops are rice and soybeans. The weather is typical of the Asian monsoon climate, which is characterized by a long winter–spring dry season followed by a summer–early autumn rainy season. The annual mean precipitation over the watershed from 2004 to 2013 was 1,408 mm, and 67% of the annual precipitation occurred between June and September.

2.3. Data collection

SWAT input includes (1) meteorological data, (2) spatial layers representing elevation, land use, and soil type of the watershed, (3) point source pollution, (4) agriculture activity, and (5) observed stream flow and nutrients concentration for model sensitivity analysis as well as calibration.

The study period is 2 years from 2012 to 2013. There are 11 rain gauge stations and 1 weather station, which measure rainfall, air temperature, wind speed, relative humidity, atmospheric pressure, and solar intensity. The meteorological data are measured with a 1-min time interval; they were provided by the Korea Meteorological Administration (KMA). Radar rainfall during the study period was collected from the constant altitude plan position indicator (CAPPI) operated by KMA. CAPPI is the synthesized image of the cloud monitoring at a constant altitude (1.5 km) by radar monitoring stations nationwide. The radar image is obtained in a grid format at the 4 km^2 (2 km × 2 km) spatial resolution, with a 10-min interval. All the meteorological data were converted to daily time steps.

Topographical, land use, and soil type data were obtained from the online water management information system (WAMIS) managed by the Ministry of Land, Infrastructure and Transport (MOLIT). Annual discharge flow and pollutant load of four wastewater treatment plants on the YR were acquired from the Ministry of Environment (ME). The agriculture activity database was acquired from the Korea rural development administration, and it included the timing of tillage operation, fertilizer application, planting/beginning of growing season, harvest and kill operation, quantity of fertilizer applied, and method of tillage. Daily stream flow data are derived at the Hampyeong (HP) hydrometric station, operated by MOLIT, located 45 km upstream from the outlet of Yeongsan River to minimize the effects of tides on hydrographs. Weekly concentration of total suspended solid and total phosphorus at the HP site was obtained from ME, aggregated to monthly pollutant load by using stream flow for the SWAT model.

2.4. Rainfall estimates from weather radar images

The process of estimating rainfall intensity from weather radar is divided into three phases. Phase I derives rainfall estimates from color distribution in weather radar images. Rainfall intensity is converted from 10-min interval to daily interval. Phase II estimates the correction factor to convert rainfall estimates from Phase I to those with daily rain gauge observations. In Phase III, the corrected radar rainfall estimates of each grid cell was obtained by applying the correction factor from Phase II to rainfall estimates from Phase I. Phase III rainfall estimates are supposed to be more accurate than Phase I estimates, and can also estimate the rainfall intensity of ungauged sub-basins because weather radar covered the entire Korean Peninsula.

In Phase I, weather radar images provided from KMA were subjected to the weather radar image processing in a MATLAB environment. The characteristics of color in the grids of the total radar images were converted to rainfall estimates through weather radar image processing, and the standard for the conversion is the standard index provided in the weather radar image. After weather radar image processing, rainfall intensity (mm/h) at the time of image acquisition is assigned to each grid cell. The rainfall intensity provided at intervals of 10 min was aggregated in these grids to obtain daily rainfall intensity (mm/d). Weather radar images were collected during 2 years from January 2012 to December 2013 (731 d) with 10-min interval; more than 100,000 weather radar images were analyzed.

In Phase II, the mean field bias correction (MFBC) method was applied for improving the quality of rainfall estimates from the weather radar images. This rainfall bias correction method has been used by several researchers [12,23]. The correction factor based on the MFBC method is calculated using the ratio of the spatial averages of rain gauge observations and rainfall estimates from weather radar images at a corresponding point. The equation of the MFBC method is as follows:

$$\text{Correction factor} = \sum_{i=1}^{n} G_i \Big/ \sum_{i=1}^{n} R_i \tag{1}$$

where G_i is the rainfall observation of the ith rain gauge, R_i is the rainfall estimates of the ith point from the radar, and n is the total number of the ground rain gauge. In YRW, there are 11 ground rain gauges. Therefore, the rainfall estimates from the weather radar images at corresponding points with 11 ground rain gauges were extracted.

In Phase III, the identical correction factor calculated from Phase II can be applied uniformly to rainfall estimates from radar images all over the area. Thus, this study obtained the corrected rainfall estimates of 25 points that are at the center of YRW sub-basins.

To compare the model prediction accuracy under different composition of rainfall inputs, three different rainfall input datasets were constructed. The first input dataset encompassed rainfall observed from 11 ground rain gauges (GR). The second input dataset was constructed only using 25 corrected rainfall estimates from weather radar images (RR). The third input dataset was constructed by combining the 11 observed rainfall with 16 corrected rainfall estimates that represent the 16 ungauged sub-basins in YRW (GARR). Then, the SWAT model was developed by using the different composition of rainfall inputs (GR, RR, and GARR), and individual sensitivity analysis and calibration was conducted.

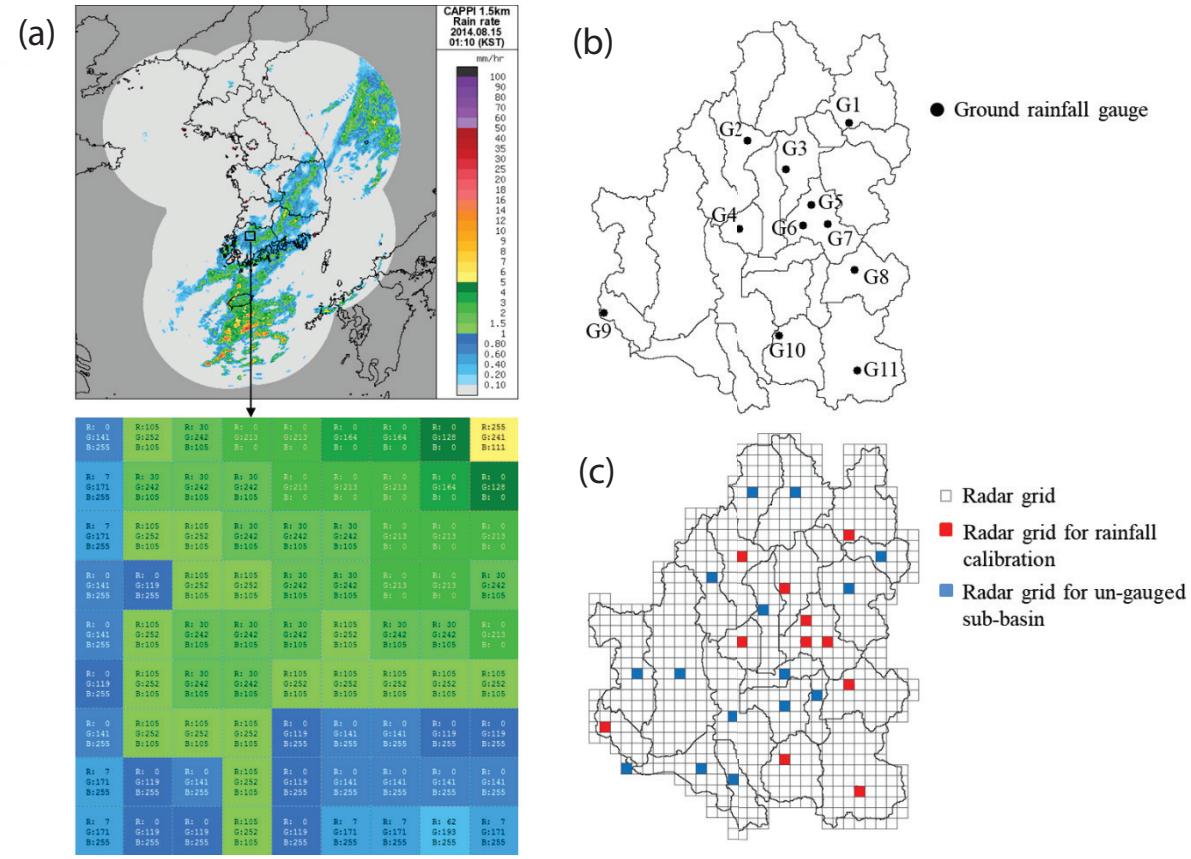

Fig. 2. Weather radar information. (a) Gridded color distribution representing rainfall intensity (mm/h) produced by weather radar image. (b) Map of ground rainfall gauges. (c) Map of selected radar image grids to calibrate of rainfall produced by weather radar images and to estimate the rainfall intensity at ungauged sub-basins.

The SWAT model developed by GR was simulated using rainfall data from nine ground rainfall gauges because the locations of G3, G6, and G7 are in the same sub-basin (Fig. 2). Therefore, sub-basins of 16 that do not have ground rainfall gauges use the weather station nearest to the center in each sub-basin.

2.5. Sensitivity analysis and model calibration

The sensitivity analysis and calibration of the SWAT model were performed to predict daily stream flow, monthly TSS load, and monthly TP load during 2 years (2012–2013) at HP station (Fig. 1). A sensitivity analysis on model parameters was performed based on the Latin-Hypercube One-factor-At-a-Time (LH-OAT). The LH simulation, as an alternative to Monte Carlo sampling, selects random values over the parameter space [24]. Through the sensitivity analysis, significant parameters for calibrating the SWAT model were determined.

For automatic calibration of stream flow, the ParaSol method, provided by ArcSWAT interface, was applied to acquire the optimal parameter value. The SWAT model was calibrated for predicting monthly TSS load and monthly TP load by using the pattern search method. The Nash–Sutcliffe efficiency (NSE) coefficient was used to evaluate model prediction accuracy [25]. The statistical hypothesis test on the efficiency index was applied to compare the model performance for predicting stream flow and nutrient load [26]. Percentage bias (PBIAS) was also used for interpreting the average tendency of simulations to be over- or under-estimated compared with observations [27].

3. Results and discussion

3.1. Radar rainfall estimation

Raw rainfall estimations produced by weather radar images have limitations for direct application to the watershed model because uncorrected rainfall estimates lead to substantially underestimated thresholds [28]. Therefore, the MFBC method for correcting the raw rainfall estimations was used. Rainfall estimates of 11 grids, which overlap with ground rain gauges in the weather radar images, are bias-corrected ground rainfall observations; the radar rainfall estimation accuracy was assessed by comparison with ground rainfall observations at a corresponding point. Fig. 3 shows the scatter plots with linear regression equation and coefficient of regression between corrected radar rainfall estimates and ground rainfall observations for all ground rain gauges. The slopes of the linear regression equation are less than 1, except for G10; this means that the MFBC method successfully corrected the rainfall estimates from radar but did not completely improve the underestimation of

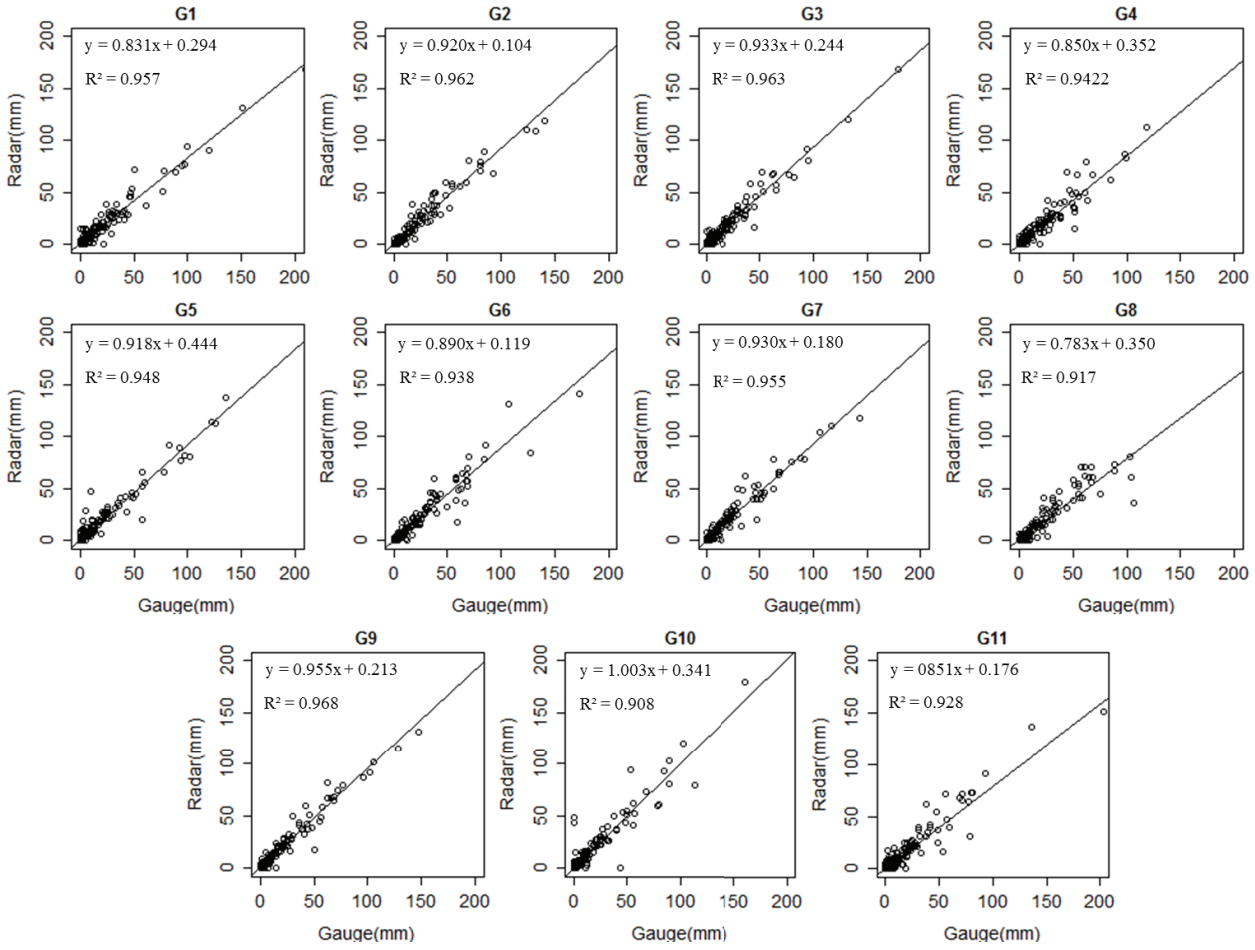

Fig. 3. Comparison of calibrated radar rainfall estimates with ground rainfall observations from gauge stations.

rainfall estimates compared with the ground rainfall observations. When we also compared the log-transformed rainfall intensities, the radar is more sensitive to very light rainfall compared with the ground gauge because the ground gauge detects rainfall at 0.5 mm unit per min, while radar can detect rainfall at 0.1 mm unit per min. These results mean that the radar rainfall estimates corrected by MFBC method describe the actual rain event well; furthermore, the correction factor is acceptable to be applied to raw rainfall estimates from weather radar images for estimating rainfall intensity at ungauged sub-basins.

3.2. SWAT model calibration

The sensitivity analysis was performed to assess the relative contribution of a set of parameters to predictions of daily flow discharge, monthly TSS load, and monthly TP load. The sensitivity analysis results and selected parameters are presented in Table 1. Sensitivity analysis was performed using 26 stream flow, 7 sediments, and 14 TP parameters. The most sensitive parameter for prediction of flow discharge using GR was SCS runoff curve number for moisture condition 2 (CN2), followed by ALPHA_BF, CH_K2, SURLAG, CH_N2, GWQMN, and ESCO. In case of RR and GARR, the rank of sensitivity was changed; baseflow alpha factor (ALPHA_BF) was the most sensitive parameter. The calibration of daily stream flow was conducted using the top seven parameters based on the results of sensitivity analysis (Table 1). The CN2 value was initially set based on the parameter given the land use, soil, and slope at each HRU, and was calibrated by a factor ranging from –25 to 25. The CN2 value using GR data was calibrated to a negative skew; this means that infiltration was increased. A positive skew was observed in RR and GARR data; this means that the overland flow was increased [29]. These differences are because the corrected radar rainfall estimates were relatively underestimated compared with the ground gauge rainfall. The most sensitive parameter for TSS load simulation using GR data was the coefficient in sediment transport equation (SPCON), followed by PRF, CH_COV, and USLE_P. The peak rate adjustment factor (PRF) was considered the most sensitive for the SWAT model using RR and GARR data. These sediment parameters were used to compute the amount of TSS load from the catchment and channel. The calibration parameters showed no big differences between the three rainfall data. This was because the main parameters for predicting TSS load affect channel erosion processes. The most sensitive parameter for TP load simulation using GR data was phosphorus enrichment ratio concentration of soluble phosphorus (ERORGP), followed by BIOMIX, PSP, BC4, GWSOLP, RHCQ, and MUMAX. The local

algal respiration rate at 20°C (RHOQ) was considered the most sensitive for the SWAT model using RR and GARR data. These seven parameters were selected for calibration.

3.3. Sensitivity to rainfall data

In this section, we examined the availability of the radar rainfall estimates from the hydrological and water quality modeling perspective. Table 2 presents a comparison of the simulation results for the daily total stream flow, daily low and high stream flow, monthly TSS load, and monthly TP load under the three different rainfall sources (GR, RR, and GARR). NSE values all confirmed that the watershed-scale and water quality model driven by the rainfall data combining the gauge rainfall and radar rainfall (GARR) performed better than those from gauge rainfall (GR) and radar rainfall (RR). Simulations of total stream flow resulted in NSE values of 0.79, 0.86, and 0.87 for GG, RR, and GARR data. Moreover, PBIAS values were 1.3%, 7.7%, and –0.7%, for GG, RR, and GARR data. In general, the performance ratings for all rainfall data were "very good" according to the general performance ratings for SWAT model shown in Table 3 [30]. Comparison of the visual inspection of GR-, RR-, and GARR-simulated stream flow indicated that SWAT simulations followed satisfactorily observed stream flow (Fig. 4). In relative terms, GARR data were shown to produce more accurate stream flow prediction than GR and RR data, according to NSE values. It was also verified that NSE values were significantly different among the SWAT models developed by GG, RR, and GARR data through hypothesis tests on the NSE value.

To examine the variation in stream flow simulation results according to rainfall data source, the simulation accuracy was compared by subdividing data into high and low flow datasets. The standard value for classifying stream flow into high and low was calculated by adding the average value and standard deviation value of observed stream flow during the simulation period. The daily-average stream flow

Table 1
Results of sensitivity analysis and calibration of stream flow, total suspended solid (TSS) load, and total phosphorus (TP) load

Parameter	Gauge		Radar		Gauge and radar	
	Sensitivity rank	Calibration value	Sensitivity rank	Calibration value	Sensitivity rank	Calibration value
Cn2	1	–0.945	2	6.055	2	14.184
Alpha_Bf	2	0.986	1	0.984	1	0.078
Ch_K2	3	2.243	3	51.984	3	12.000
Surlag	4	8.344	4	1.109	4	1.093
Ch_N2	5	0.448	5	0.337	5	0.948
Gwqmn	6	0.586	6	997.300	6	995.425
Esco	7	0.635	7	0.006	7	0.006
SPCON	1	0.001	2	0.001	2	0.001
PRF	2	0.500	1	0.500	1	0.500
CH_COV	3	0.000	3	0.000	3	0.000
USLE_P	4	0.100	4	0.100	4	0.100
ERORGP	1	0.550	3	0.550	3	1.3434
BIOMIX	2	0.100	7	0.020	7	0.100
PSP	3	0.600	4	0.200	4	0.307
BC4	4	0.100	6	0.300	6	0.500
GWSOLP	5	0.000	2	0.825	2	0.000
RHOQ	6	0.050	1	0.050	1	0.050
MUMAX	7	1.000	5	1.000	5	2.200

Table 2
Nash–Sutcliffe efficiency (E_{NS}) and percent bias (PBIAS) for daily stream flow, monthly total suspended soil (TSS) load, and total phosphorus (TP) load during calibration period

Indicator		Gauge		Radar		Gauge and radar	
		E_{NS}	PBIAS	E_{NS}	PBIAS	*E*NS	PBIAS
Flow	Entirety	0.79	1.3	0.86	7.7	0.87	–6.5
	High	0.62	11.3	0.77	11.7	0.79	10.5
	Low	–0.29	–5.9	–0.05	4.6	0.05	–18.6
TSS	Entirety	0.87	–4.5	0.90	1.4	0.93	2.2
TP	Entirety	0.72	16.7	0.79	14.9	0.81	8.7

Table 3
General performance ratings for statistic measures

Performance rating	NSE	PBIAS (%)		
		Stream flow	TSS	TP
Very good	0.75 < NSE ≤ 1.00	PBIAS < ±10	PBIAS < ±15	PBIAS < ±25
Good	0.65 < NSE ≤ 0.75	±10 ≤ PBIAS < ±15	±15 ≤ PBIAS < ±30	±25 ≤ PBIAS < ±40
Satisfactory	0.50 < NSE ≤ 0.65	±15 ≤ PBIAS < ±25	±30 ≤ PBIAS < ±55	±40 ≤ PBIAS < ±70
Unsatisfactory	NSE ≤ 0.50	PBIAS ≥ ±25	PBIAS ≥ ±55	PBIAS ≥ ±70

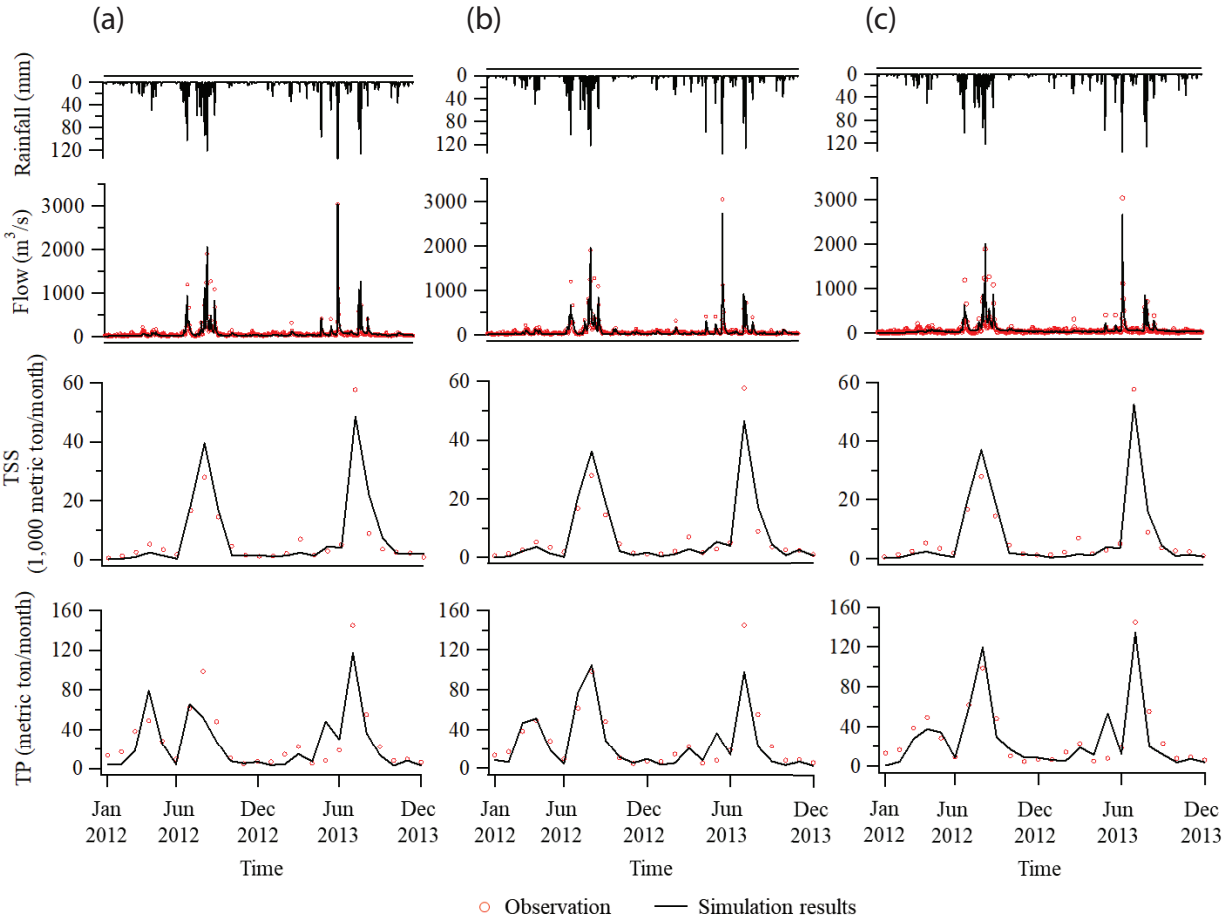

Fig. 4. Performance of the SWAT model assessed in Hampyung station during 2012 and 2013 for daily flow discharge, monthly total suspended solid load, and monthly total phosphorus load: (a) gauge rainfall (GR) data, (b) radar rainfall (RR) data, (c) gauge and radar rainfall (GARR) data.

during 2 years was 75.9 m^3/s, and the standard deviation was 188 m^3/s. According to the standard value, stream flow data of 32 d was classified as high stream flow; average value of high stream flow was 731.9 m^3/s. The stream flow data of 699 d was classified as low stream flow; average value of low stream flow was 45.9 m^3/s. All NSE values confirmed that the simulation of high stream flow performed better than that of low stream flow, regardless of the rainfall source (Table 2). These simulation results are similar to the findings in some previous studies [31,32]. Simulations of high stream flow resulted in NSE values of 0.62, 0.77, and 0.79 for GG, RR, and GARR data. The PBIAS values were 11.3%, 11.7%, and 10.5% for GG, RR, and GARR data. As a general rule, the PBIAS values indicated that the simulation of high stream flow was "good" under all rainfall data. The NSE values for RR and GARR data was also "very good" while the NSE value for GR was "good". The simulation results generally underestimated high flows according to the PBIAS values; a tendency to underestimate high stream flow of SWAT model has been observed in some published studies even when the model performance was satisfactory [33-36]. According to NSE values, GARR data produced more accurate simulated high stream flow; the hypothesis test on NSE value confirmed significant differences in NSE values between GR data and RR data as well as

between GR data and GARR data. However, there were no significant differences between RR data and GARR data. In general, the radar-driven simulation of high stream flow was better than gauge-driven simulation [18,37]. In terms of simulation of low stream flow, the NSE values were –0.29, –0.05, and 0.05 for GR, RR, and GARR data, and the PBIAS values were –5.9%, 4.6%, and –18.6%. The NSE values for all rainfall data showed unsatisfactory performance rating (NSE ≤ 0.50). The lower performance of low stream flow simulation can be described as follows. First, measurement errors in the low-flow condition may be at least twice as large as for those in the high stream flow condition [38–40]. Therefore, measurement error can affect to calibration of low stream flow. Second, SWAT model performance during low stream flow conditions is generally lower than that during high stream flow or flood conditions [31,41]. Third, the NSE value is sensitive to larger values. Consequently, the NSE value more sensitively reflects the high stream flow compared with low stream flow [41]. Nevertheless, GARR data has improved simulation accuracy of low stream flow compared to GR and RR data. On the contrary, according to the PBIAS values, the simulations of low stream flow using GR or RR data were "very good", while GARR data showed "satisfactory". The GR and GARR data showed overestimation of low stream flow, while the RR data showed an underestimation trend.

Comparison between the simulated and the observed monthly TSS load showed that the NSE values were 0.87, 0.90, and 0.93 for GR, RR, and GARR data, and the PBIAS values were –4.5%, 1.4%, and 2.2% (Table 2). The statistic measures (NSE and PBIAS) indicated that the model performance for predicting TSS load were "very good" for all rainfall data. However, when compared with each NSE value with the hypothesis test, the model performance was significantly better under GARR data than under GR and RR data. An explanation for this result is that the simulation of peak TSS load using GARR data followed the observed peak TSS load more satisfactorily when compared by visual inspection (Fig. 4). Comparison between the simulated and observed TP load showed that the NSE values under GG, RR, and GARR data were 0.72, 0.79, and 0.81, respectively (Table 2), and the PBIAS values were 16.7%, 14.9%, and 8.7%. According to the NSE value, the model performance using RR and GARR data was "very good", while the model performance using GR data was "good". It was also verified that the model performance using RR and GARR data were significantly better than that using GR data through hypothesis tests on the NSE value. However, there were no significant differences between the model performance under RR and GARR. In terms of the PBIAS value, the model performance for predicting TP load were "very good" in all rainfall data, and the GARR data showed the minimum PBIAS value. Moreover, the visual comparison of the simulated TP load indicated that the simulation result using GARR data was approximately equal with the observed TP load. Comprehensive comparison of the statistic measures showed that the rainfall data with combined gauge rainfall and corrected radar rainfall can improve the prediction accuracy for stream flow, TSS load, and TP load. The improvements to the model performance presented here should contribute to increase the prediction accuracy of water quality and quantity in response to regional climate change by using high resolution rainfall data of weather radar image.

4. Conclusion

In this study, an attempt was made to identify whether the radar rainfall data will be helpful in improving simulation performance of watershed-scale water quality model. Three different types of rainfall data for a SWAT model were constructed: gauge rainfall (GR), radar rainfall (RR), and gauge and radar rainfall (GARR). The SWAT model was developed for predicting stream flow, TSS load, and TP load at Yeongsan River, using three types of rainfall data. The main findings in this study are as follows:

- In general, the rainfall estimations produced by radar has limitations for direct application to the watershed-scale water quality model owing to the tendency of underestimation of radar rainfall. Thus, the MFBC method was applied to the raw rainfall estimations. When compared with the ground rainfall observations, the MFBC method did not completely improve the tendency of underestimation, but the radar rainfall estimates corrected by the MFBC method describe well the actual rainfall event and rainfall intensity. Therefore, the corrected radar rainfall estimates are adaptable for estimating rainfall at ungauged sub-basins.
- The SWAT model responded differently to rainfall data sets. The sensitivity rank of parameters for stream flow, TSS load, and TP load was not different under RR and GARR data; parameters under GR data showed the greatest change in rank compared with those under RR and GARR data. An explanation for this result is the ungauged sub-basins, which used radar rainfall estimates comprising a large proportion of YSW. Therefore, in the case of GARR data, the sensitivity rank of parameters is similar with that under RR data.
- The SWAT model predicted stream flow, TSS load, and TP load well during the calibration period even when using different rainfall data and optimal parameter values. In particular, GARR data are more favorable for water quantity and quality simulation in the selected watershed compared with GR and RR data. This means the watershed-scale water quality model can improve the simulation accuracy by using a new combination of gauge rainfall for gauged sub-basin and radar rainfall estimates for ungauged sub-basin.

Acknowledgements

This work was supported by GIST Research Institute (GRI) grant funded by the GIST in 2018.

References

[1] D. Borah, M. Bera, Watershed-scale hydrologic and nonpoint-source pollution models: review of mathematical bases, Trans. ASAE, 46 (2003) 1553.
[2] R. Jamieson, R. Gordon, D. Joy, H. Lee, Assessing microbial pollution of rural surface waters: a review of current watershed scale modeling approaches, Agric. Water Manage., 70 (2004) 1–17.
[3] E.G. Bekele, H.V. Knapp, Watershed modeling to assessing impacts of potential climate change on water supply availability, Water Resour. Manage., 24 (2010) 3299–3320.
[4] K. Price, Effects of watershed topography, soils, land use, and climate on baseflow hydrology in humid regions: a review, Prog. Phys. Geogr., 35 (2011) 465–492.

[5] C. Wellen, A.-R. Kamran-Disfani, G.B. Arhonditsis, Evaluation of the current state of distributed watershed nutrient water quality modeling, Environ. Sci. Technol., 49 (2015) 3278–3290.
[6] K.H. Cho,Y.A. Pachepsky, J.H. Kim, J.-W. Kim, M.-H. Park, The modified SWAT model for predicting fecal coliforms in the Wachusett Reservoir Watershed, USA, Water Res., 46 (2012) 4750–4760.
[7] M. Geza, J.E. McCray, Effects of soil data resolution on SWAT model stream flow and water quality predictions, J. Environ. Manage., 88 (2008) 393–406.
[8] I. Chaubey, A. Cotter, T. Costello, T. Soerens, Effect of DEM data resolution on SWAT output uncertainty, Hydrol. Process, 19 (2005) 621–628.
[9] J.-M. Faurès, D. Goodrich, D.A. Woolhiser, S. Sorooshian, Impact of small-scale spatial rainfall variability on runoff modeling, J. Hydrol., 173 (1995) 309–326.
[10] M. Yu, X. Chen, L. Li, A. Bao, M.J. De la Paix, Streamflow simulation by SWAT using different precipitation sources in large arid basins with scarce raingauges, Water Resour. Manage., 25 (2011) 2669.
[11] V. Neary, E. Habib, M. Fleming, Hydrologic modeling with NEXRAD precipitation in middle Tennessee, J. Hydrol. Eng., 9 (2004) 339–349.
[12] L. Kalin, M.M. Hantush, Hydrologic modeling of an eastern Pennsylvania watershed with NEXRAD and rain gauge data, J. Hydrol. Eng., 11 (2006) 555–569.
[13] S. Eleuch, A. Carsteanu, K. Bâ, R. Magagi, K. Goïta, C. Diaz, Validation and use of rainfall radar data to simulate water flows in the Rio Escondido basin, Stochastic Environ. Res. Risk Assess., 24 (2010) 559–565.
[14] A. Elhassan, H. Xie, A.A. Al-othman, J. Mcclelland, H.O. Sharif, Water quality modelling in the San Antonio River Basin driven by radar rainfall data, Geomatics, Geomat. Nat. Hazards Risk, 7 (2016) 953–970.
[15] R. Jayakrishnan, R. Srinivasan, C. Santhi, J. Arnold, Advances in the application of the SWAT model for water resources management, Hydrol. Process., 19 (2005) 749–762.
[16] P.-A. Versini, Use of radar rainfall estimates and forecasts to prevent flash flood in real time by using a road inundation warning system, J. Hydrol., 416 (2012) 157–170.
[17] S. Rozalis, E. Morin, Y. Yair, C. Price, Flash flood prediction using an uncalibrated hydrological model and radar rainfall data in a Mediterranean watershed under changing hydrological conditions, J. Hydrol., 394 (2010) 245–255.
[18] J.P. Looper, B.E. Vieux, An assessment of distributed flash flood forecasting accuracy using radar and rain gauge input for a physics-based distributed hydrologic model, J. Hydrol., 412 (2012) 114–132.
[19] W. Yu, E. Nakakita, S. Kim, K. Yamaguchi, Improvement of rainfall and flood forecasts by blending ensemble NWP rainfall with radar prediction considering orographic rainfall, J. Hydrol., 531 (2015) 494–507.
[20] J.G. Arnold, R. Srinivasan, R.S. Muttiah, J.R. Williams, Large area hydrologic modeling and assessment part I: model development, JAWRA, 34 (1998) 73–89.
[21] M. Gitau, T. Veith, W. Gburek, Farm–Level Optimization of BMP Placement for Cost–Effective Pollution Reduction, Trans. ASAE, 47 (2004) 1923.
[22] K.C. Abbaspour, J. Yang, I. Maximov, R. Siber, K. Bogner, J. Mieleitner,J . Zobrist, R. Srinivasan, Modelling hydrology and water quality in the pre-alpine/alpine Thur watershed using SWAT, J. Hydrol., 333 (2007) 413–430.
[23] J.-K. Lee, J.-H. Kim, M.-K. Suk, Application of bias correction methods to improve the accuracy of quantitative radar rainfall in Korea, Atmos. Meas. Tech., 8 (2015) 4011–4047.
[24] M.D. McKay, R.J. Beckman, W.J. Conover, Comparison of three methods for selecting values of input variables in the analysis of output from a computer code, Technometrics, 21 (1979) 239–245.
[25] J.E. Nash, J.V. Sutcliffe, River flow forecasting through conceptual models part I—A discussion of principles, J. Hydrol., 10 (1970) 282–290.
[26] R.H. McCuen, Z. Knight, A.G. Cutter, Evaluation of the Nash–Sutcliffe efficiency index, J. Hydrol. Eng., 11 (2006) 597–602.
[27] H.V. Gupta, S. Sorooshian, P.O. Yapo, Status of automatic calibration for hydrologic models: comparison with multilevel expert calibration, J. Hydrol. Eng., 4 (1999) 135–143.
[28] F. Marra, E.I. Nikolopoulos, J.D. Creutin, M. Borga, Radar rainfall estimation for the identification of debris-flow occurrence thresholds, J. Hydrol., 519 (2014) 1607–1619.
[29] K. Price, S.T. Purucker, S.R. Kraemer, J.E. Babendreier, C.D. Knightes, Comparison of radar and gauge precipitation data in watershed models across varying spatial and temporal scales, Hydrol. Process, 28 (2014) 3505–3520.
[30] D.N. Moriasi, J.G. Arnold, M.W. Van Liew, R.L. Bingner, R.D. Harmel, T.L. Veith, Model evaluation guidelines for systematic quantification of accuracy in watershed simulations, Trans. ASABE, 50 (2007) 885–900.
[31] D. Zhang, X. Chen, H. Yao, B. Lin, Improved calibration scheme of SWAT by separating wet and dry seasons, Ecol. Modell., 301 (2015) 54–61.
[32] K. Price, S.T. Purucker, S.R. Kraemer, J.E. Babendreier, Tradeoffs among watershed model calibration targets for parameter estimation, Water Resour. Res., 48 (2012) 10.
[33] N. Kannan, S. White, F. Worrall, M. Whelan, Hydrological modelling of a small catchment using SWAT-2000–Ensuring correct flow partitioning for contaminant modelling, J. Hydrol., 334 (2007) 64–72.
[34] M. Larose, G. Heathman, L. Norton, B. Engel, Hydrologic and atrazine simulation of the Cedar Creek watershed using the SWAT model, J. Environ. Qual., 36 (2007) 521–531.
[35] A. Stehr, P. Debels, F. Romero, H. Alcayaga, Hydrological modelling with SWAT under conditions of limited data availability: evaluation of results from a Chilean case study, Hydrol. Sci. J., 53 (2008) 588–601.
[36] L.-j. Qiu, F.-l. Zheng, R.-s. Yin, SWAT-based runoff and sediment simulation in a small watershed, the loessial hilly-gullied region of China: capabilities and challenges, Int. J. Sediment Res., 27 (2012) 226–234.
[37] J. Moon, R. Srinivasan, J. Jacobs, Stream flow estimation using spatially distributed rainfall in the Trinity River basin, Texas, Trans. ASAE, 47 (2004) 1445.
[38] G. Di Baldassarre, A. Montanari, Uncertainty in river discharge observations: a quantitative analysis, Hydrol. Earth Syst. Sci., 13 (2009) 913.
[39] D.M. Thomas, M.A. Benson. Generalization of Streamflow Characteristics from Drainage-Basin Characteristics, US Government Printing Office Washington, D.C., 1970.
[40] K. Eng, P. Milly, Relating low-flow characteristics to the base flow recession time constant at partial record stream gauges, Water Resour. Res., 43 (2007) 1.
[41] H. Li, M. Sivapalan, F. Tian, Comparative diagnostic analysis of runoff generation processes in Oklahoma DMIP2 basins: the Blue River and the Illinois River, J. Hydrol., 418 (2012) 90–109.